AIP | Applied Physics Letters

Effects of configurational changes on molecular dynamics in polyvinylidene fluoride and poly(vinylidene fluoride-trifluoroethylene) ferroelectric polymers

N. Jalarvo, A. Pramanick, C. Do, and S. O. Diallo

Citation: Applied Physics Letters **107**, 082907 (2015); doi: 10.1063/1.4929693
View online: http://dx.doi.org/10.1063/1.4929693
View Table of Contents: http://scitation.aip.org/content/aip/journal/apl/107/8?ver=pdfcov
Published by the AIP Publishing

Effects of configurational changes on molecular dynamics in polyvinylidene fluoride and poly(vinylidene fluoride-trifluoroethylene) ferroelectric polymers

N. Jalarvo,[1,2,a)] A. Pramanick,[3,a)] C. Do,[4] and S. O. Diallo[2,a)]
[1]*Jülich Centre for Neutron Science, Forschungszentrum Jülich GmbH, 52428 Jülich, Germany*
[2]*Chemical and Engineering Materials Division, Oak Ridge National Laboratory, Oak Ridge, Tennessee 37831, USA*
[3]*Department of Physics and Materials Science, City University of Hong Kong, Kowloon, Hong Kong*
[4]*Biology and Soft-Matter Division, Oak Ridge National Laboratory, Oak Ridge, Tennessee 37831, USA*

(Received 19 May 2015; accepted 16 August 2015; published online 28 August 2015)

We present a comparative study of proton dynamics in unpoled non-ferroelectric polymer polyvinylidene fluoride (PVDF) and in its trifluoroethylene containing ferroelectric copolymer (with 70/30 molar proportion), using quasi-elastic neutron scattering. The neutron data reveal the existence of two distinct types of molecular motions in the temperature range investigated. The slower motion, which is characterized in details here, is ascribed to protons jump diffusion along the polymeric carbon chains, while the faster motion could be attributed to localized rotational motion of methylene groups. At temperatures below the Curie point ($T_c \sim 385$ K) of the composite polymer, the slower diffusive mode experiences longer relaxation times in the ferroelectric blend than in the bare PVDF, although the net corresponding diffusion coefficient remains comparatively the same in both polymers with characteristic activation energy of $E_A \approx 27$–33 kJ/mol. This arises because of a temperature dependent jump length r_0, which we observe to be effectively longer in the copolymer, possibly due to the formation of ordered ferroelectric domains below T_c. Above T_c, there is no appreciable difference in r_0 between the two systems. This observation directly relates the known dependence of T_c on molar ratio to changes in r_0, providing fundamental insight into the ferroelectric properties of PVDF-based copolymers. © *2015 AIP Publishing LLC*.
[http://dx.doi.org/10.1063/1.4929693]

Ferroelectric polymers are attractive due to their high-flexibility, low production cost, and easy integration with silicon-based and organic electronics. Owing to their remarkable ferroelectric and electromechanical properties, poly(vinylidene fluoride) (PVDF), and its copolymers with trifluoroethylene (TrFE) or tetrafluoroethylene, are considered for actuators, non-volatile memories, organic thin-film transistors, high-power-density capacitors, and energy-harvesting.[1–8] The functional properties of these polymers depend largely on their crystal phases, which are characterized by different conformations of hydrogen and fluorine atoms around long-chain carbon backbones. In unpoled state, PVDF exists in the lowest energy α-phase, which is nonpolar and has a combination of trans(T) and gauche(G) bonds packed in antiparallel fashion (Figure 1(a)). When PVDF is copolymerized with other fluoropolymers, the presence of additional fluorine atoms leads to different conformations and polarization characteristics. For example, the additional F atoms in P(VDF-TrFE) causes an increased stabilization of the β-phase that has an all-trans(TTTT) configuration[9–11] and has a net ferroelectric polarization at room temperature (RT) (see Figure 1(b)). Changes in relative proportions of T and G bonds are also caused by temperature or external electric fields.[10,12] In order to better design ferroelectric copolymers for applications in high-frequency devices and variable environments, it is important to understand the effects of such configurational changes on dynamics of mesoscopic molecular motions. Dielectric spectroscopy and dynamic mechanical analysis elucidated the relaxation times for PVDF copolymers in the macroscopic time scales of $t \geq 10^{-6}$ s (or frequency, $f \leq 10^6$ Hz).[13–15] At the other end of the spectrum, Raman and IR spectroscopies provided insights into how atomistic vibrational dynamics in PVDF polymer chains in sub-picoseconds time scale (or $f \geq 10^{12}$ Hz) are altered by different configurations.[16–18] In comparison, the effects of configurational changes on relaxational dynamics in PVDF-copolymers at picoseconds-to-nanoseconds are not well understood, although such motions play critical roles in phase transition and switching behaviors.

Quasielastic-neutron-scattering (QENS) is an excellent technique for characterizing relaxational dynamics in polymers in the picoseconds-to-nanoseconds time-scale.[19,20] Application of QENS to study PVDF-copolymers has been rather limited, in comparison to other spectroscopic techniques. Earlier QENS studies of P(VDF-TrFE)[21,22,31,32] revealed the nature of molecular motions, such as (a) a vibrational motion of Debye-Waller type, (b) a slow jump diffusive motion within confined volumes, and (c) a fast localized rotational diffusive motion. These co-polymers are typically semi-crystalline with average crystallinity of ∼70%.[32] All these motions showed characteristic changes during ferroelectric-to-paraelectric phase transition. However, for same temperatures both below and above the T_C, the differences in relaxational dynamics between an all-T configuration and a mixed state of T and G bonds are not entirely clear. Here, using comparative analysis of QENS spectra in α-PVDF and

[a)]Authors to whom correspondence should be addressed. Electronic addresses: jalarvonh@ornl.gov, abhijit.pramanick@gmail.com, and omardiallos@ornl.gov.

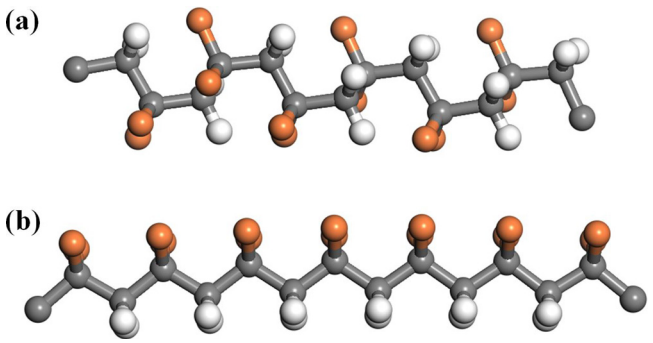

FIG. 1. Schematic for arrangement of hydrogen and fluorine (white and orange spheres) around the carbon (grey spheres) backbone in PVDF polymer (a) trans and gauche conformation and (b) all-trans conformation.

70/30 P(VDF-TrFE) copolymer, we examined the effect of stabilizing an all-trans configuration on the dynamics of molecular motions at picoseconds-to-nanoseconds timescale. While α-PVDF has alternating T and G bonds, an all-T configuration is stabilized in the P(VDF-TrFE) copolymer, which can have up to 75% crystalline chains in polar all-T configuration as reported for 68 mol. % VDF content.[4,23] Both experimental[24] and theoretical studies[10] indicate that during ferroelectric-paraelectric phase transition conformational changes in the P(VDF-TrFE) copolymer occur only in the VDF segment, while no changes occur at the position of the TrFE monomer. Therefore, for comparative analysis of the two polymers, differences in their QENS spectra should majorly originate from the altered configurations of their $(CH_2\text{-}CF_2)$- segments.

The relaxation mechanisms in PVDF-copolymers were studied by QENS at the BASIS backscattering-spectrometer of the Spallation Neutron Source (SNS) at the Oak Ridge National Laboratory (ORNL).[25] BASIS utilizes Si(111) crystal analyzers to Bragg-select neutrons scattered off the sample at various angles. The wavelength of the incoming neutron beam is centered at 6.4 Å yielding an accessible dynamic range free from spurious background from -100 to $+100\,\mu$eV, and an energy-resolution at the elastic peak of $\sim 3.4\,\mu$eV (full-width-at-half-maximum). The data were selectively summed together into 9 Q-bins, from 0.2 to 2.0 Å^{-1}, in equal steps of 0.2 Å^{-1}. Coherent Bragg scattering was found between 1.2 and 1.4 Å^{-1}, thus that Q region was excluded from analysis.

The polymer samples were purchased from Piezotech, S.A.S. (France). As per supplier provided documentation, the Curie (T_C) and melting (T_M) temperatures of the P(VDF-TrFE) copolymer are ~385 K and ~429 K, respectively. For the PVDF film, the T_M is ~448 K. T_C for PVDF is estimated to be ~473 K;[26] however, since it is more than T_M, T_C is not observed experimentally. The remnant polarization for the ferroelectric P(VDF-TrFE) film is $\sim 9\,\mu\text{C/cm}^2$, which is consistent with earlier reported values.[1,4,23,27] For further thermal and electrical characteristics of the polymer films, the reader is referred to supplier documentation[28] and existing reviews such as Refs. 4, 23, and 29. The as-received samples were sealed into an annular Al can, and the QENS spectra were recorded at various temperatures, between 20 and 400 K. High-statistical-quality QENS data were collected at 300, 340, 370, and 400 K. The polymer films are approximately 40 μm thick, so that multiple scattering effects in these highly hydrogenous materials are minimized. The lowest temperature dataset (20 K), in which all observable molecular dynamics become resolution limited, was used to represent the instrumental resolution function. RT data collected from annular vanadium were used to normalize the data against variability in the detector efficiency.

Since the incoherent scattering cross-sections of C and F are nearly zero, and that of H is ~80 barns (10^{-24} cm^2), the QENS response arise exclusively from H dynamics. For estimating the range where measurable H dynamics set in, the temperature-dependent elastic-incoherent-neutron-scattering (EINS) contribution was calculated by integrating the measured spectra around the zero-energy-transfer line ($\omega = 0$) from -3.5 to $3.5\,\mu$eV. In Figure 2, this so-derived EINS for both PVDF and P(VDF-TrFE) are shown for Q of (a) 0.5 and (b) 1.7 Å^{-1}, corresponding to molecular length-scale of about 12 and 3.7 Å, respectively. EINS decreases with increasing temperatures as vibrational states get populated (described by Debye-Waller factor) and more rapidly when anharmonic vibrations, localized or long-range diffusive motions, become apparent in the measured time-scale. The decrease in EINS with increasing temperature is significantly more at high-Q than at low-Q. A slight change in slope of EINS at ~160 K and another well-defined transition at ~300 K can be noticed. A lattice stiffening phase transition due to local charge fluctuations was reported earlier in P(VDF-TrFE) films,[30] which is likely the cause for the transition observed here at ~160 K. The change in the slope of EINS at ~300 K arises from the diffusive dynamics of the protonated side-groups. This second transition, which is closer to T_C for P(VDF-TrFE), is observable at the entire measured Q range. The decrease in EINS above 300 K is significantly larger for P(VDF-TrFE) than for PVDF. EINS for P(VDF-TrFE) also shows a larger thermal hysteresis. Thermal hysteresis in PVDF-copolymers is associated with anharmonicity of the vibrational motion of protons attached to the main carbon chain, which likely originates from dipole-dipole interactions.[31,32] Therefore, the larger hysteresis in P(VDF-TrFE) as compared to PVDF for same temperatures is interpreted as a result of greater dipole interactions in P(VDF-TrFE), which is a consequence of stabilized all-T configuration in the copolymer.[9]

The rapid decrease in EINS for $T \geq 300$ K for both polymers indicates onset of thermally-activated diffusive processes on time-scales that are observable on the spectrometer. This is seen as a relative increase in the QE scattering, as illustrated for PVDF in Figure 3 for selected temperatures of 20, 300, and 400 K at $Q = 1.7$ Å^{-1}. The 20 K data represent the instrumental resolution, whereas the 300 and 400 K data show the temperature-dependent QE broadening. As the elastic peak intensity decreases with increasing temperatures, the QE broadening of the spectra becomes obvious. Since analysis of EINS is primarily used for diagnostic purposes, a detailed analysis of the QENS spectra is followed to evaluate the actual characteristics of the polymer dynamics.

Dynamics of the PVDF and P(VDF-TrFE) samples can be analyzed from QENS measurements at temperatures where the motions fall within the spectrometer time window (approximately picoseconds-to-nanoseconds). The EINS data indicate that a significant portion of the protons

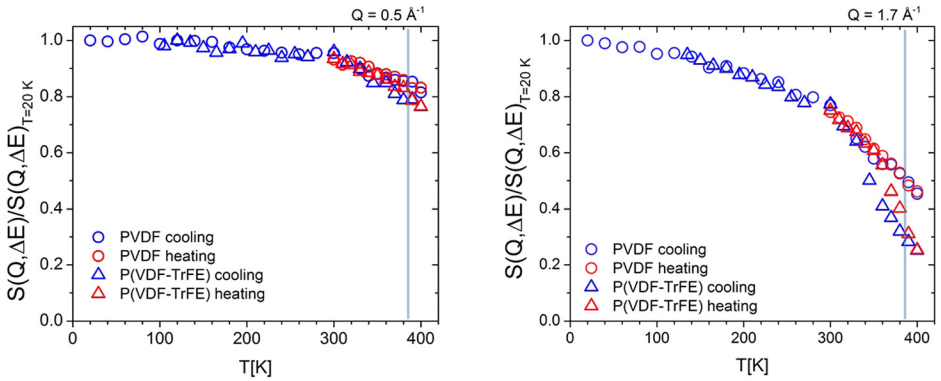

FIG. 2. Temperature dependence of the elastic intensity (EINS) at two selected Q values, 0.5 (left figure) and 1.7 Å^{-1} (right figure). The circles represent the EINS for PVDF and the triangles that of PVDF-TrFE. The colors blue and red differentiate between the cooling and heating sequences, respectively. The vertical lines show the Tc for the PVDF-TrFe (70/30) sample. A clear hysteresis in the EINS is observed at high Q, where localized dynamics are dominant.

contribute to the broadening of the QENS signal above 300 K. To gain further insights into the molecular motions, we fitted the QENS spectra at each Q to the following $S(\omega)$ model convoluted with the instrument resolution function $R(\omega)$ in the energy ω domain

$$S(\omega) = f\left[A_0\delta(\omega) + (1-A_0)\sum_{i=1}^{n} p_i \frac{1}{\pi}\frac{\Gamma_i}{\omega^2+\Gamma_i^2}\right] \otimes R(\omega) + B(\omega), \quad (1)$$

where f is a scaling factor, A_0 is the elastic scattering fraction of the total scattering, and p_i the spectral weight of the ith quasielastic (QENS) component. The spectra at 20 K (where no diffusive processes can be observed within the measured time-scale) are used as the resolution function $R(\omega)$. $B(\omega)$ is an adjustable linear background term. For the present data, we found it necessary to use two Lorentzian components ($n = 2$), each of which can be associated with one of the dynamical processes identified above. However, only processes occurring on picosecond-to-nanosecond timescales can be fully observed, and consequently reliably interpreted. To distinguish between the two observed components, we denote the halfwidth-at-half-maximum of the broader and the narrower components by Γ_{fast} and Γ_{slow}, respectively.

Figure 4 shows the A_0, Γ_{fast}, and Γ_{slow}, for the two different polymers. A clear decrease in A_0 with increasing Q is observed at all temperatures. Γ_{fast} are about an order of magnitude larger than Γ_{slow} and appears to be Q-independent, indicating a dynamical process that is localized in nature. This type of fast, localized motion can be attributed to methylene rotations. The determination of Γ_{fast} is less reliable, with randomly scattered values with respect to Q and large error bars. Low energy vibrational/librational modes contribute to this dynamics[21,22,31,32] and since they are not fully described by the model, we cannot reliably draw conclusions on the temperature dependence of Γ_{fast}. However, we

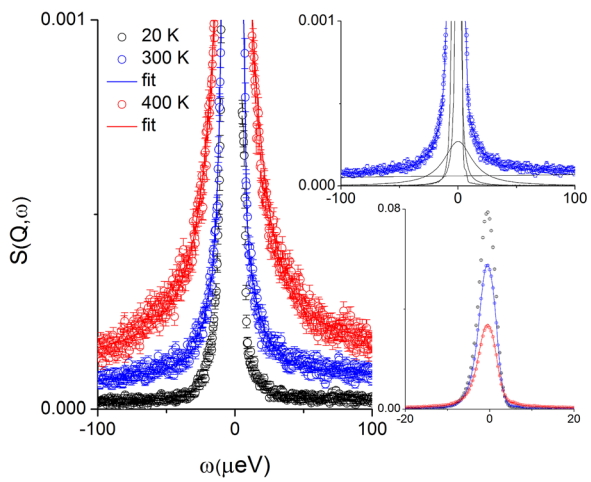

FIG. 3. Representative QENS spectra for PVDF at three selected temperatures 20, 300 and 400 K, at momentum transfer Q = 1.7 Å^{-1}. The 20 K data represents the instrument resolution function. Fits of the Eq. (1) are printed with solid lines. The intensity scale was purposefully chosen to highlight the QE contribution. The full spectra are shown over the full intensity range in the bottom inset, and fit including all the fit components (elastic peak, 2 Lorentzian functions, and flat background term) for the 300 K data is shown in the top inset.

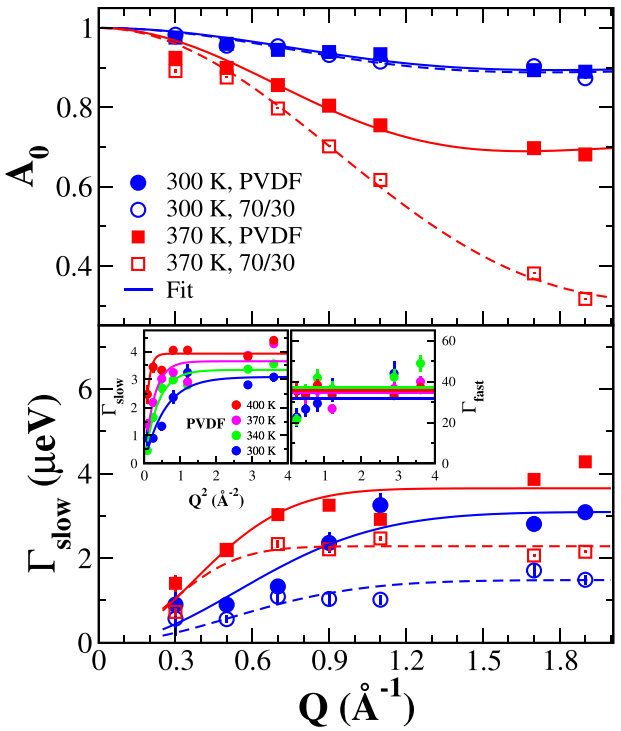

FIG. 4. Top panel: A_0 in PVDF (closed symbols) and 70/30 P(VDF-TrFE) (open symbols) plotted as a function of momentum transfer Q at two selected temperatures (300 and 370 K). Lines are fits of Eq. (3). Bottom panel: Representative plots of the width Γ_{slow} as a function of Q for the same temperatures. The insets show the full temperature dependence of the observed QENS widths as a function of Q^2, with a Γ_{slow} that is consistent with a jump-type diffusive motion (lines are fits of Eq. (3)) and a Γ_{fast} (Q) that is largely independent of Q.

TABLE I. Results of Eqs. (2) and (3) fits to the data.

T(K)	L(Å)		$(1\text{-}c_1)$		r_0(Å)	
	PVDF	P(VDF-TrFE)	PVDF	P(VDF-TrFE)	PVDF	P(VDF-TrFE)
300	3.53 ± 0.04	3.61 ± 0.04	0.11 ± 0.01	0.12 ± 0.01	1.85 ± 0.50	1.96 ± 0.50
340	3.55 ± 0.12	3.03 ± 0.08	0.22 ± 0.03	0.30 ± 0.02	2.31 ± 0.50	2.34 ± 0.55
370	3.77 ± 0.08	2.81 ± 0.11	0.32 ± 0.02	0.69 ± 0.01	2.72 ± 0.40	3.73 ± 0.70
400	15.04 ± 1.50	3.21 ± 0.45	0.66 ± 0.03	0.91 ± 0.02	4.46 ± 0.35	3.88 ± 0.25

observe a clear systematic dependence of Γ_{slow} on temperature, which we discuss below.

The advantage of QENS over other spectroscopy techniques is due to the momentum-transfer (Q) dependence of QENS spectra and possibility to extract geometrical details of the diffusion process. For instance the Q–dependence of A_0 can be studied to estimate the protons fraction diffusing along the carbon backbone within a cylinder of length L. The following expression[33] was fitted to the A_o values obtained from the fits of Eq. (1):

$$A_0 = c_1 + (1 - c_1) j_0^2 \left(\frac{QL}{2}\right), \tag{2}$$

where $j_0(x)$ is the spherical Bessel function of first kind, and $(1–c_1)$ is the fraction of protons diffusing in the cylindrical volume. Selected $A_0(Q)$ data and fits to Eq. (2) are shown in Figure 4. L and $(1\text{-}c_1)$ are listed in Table I. We find $L \sim 3$ Å in both polymers. A minor trend can be noted where L decreases with increasing temperatures for the copolymer up to 370 K, which is opposite for the bare PVDF. At 400 K, L increases greatly for PVDF ($L > 10$ Å). Since both polymers have comparable T_M above 400 K, we conclude that the random network of ferroelectric ordered domains, which is absent in the paraelectric phase, sets the size of confinement. The protons fraction diffusing in the cylindrical volume $(1\text{-}c_1)$ is smaller in PVDF than in P(VDF-TrFE) at all temperatures, except perhaps at 300 K, where c_1 and L are similar for both samples. $(1\text{-}c_1)$ increases from 11% at 300 K to 66% at 400 K in PVDF, and from 12% to than 91% in P(VDF-TrFE) over the same temperature gradient. This is understood in the light of an earlier work,[21] where two diffusion processes were described; (i) diffusion below the paraelectric transition temperature involving both amorphous and crystalline regions in the sample, for which the number of diffusing protons increases with increasing temperature, and (ii) diffusion in the paraelectric phase involving crystalline regions. Accordingly, it is apparent that at T = 300 K both samples exhibit similar characteristics. When entering the phase transition region, contributions from the paraelectric crystalline domains lead to increasing fraction of diffusing protons for the copolymer.

In Figure 4, we show Γ_{slow}, which exhibits a strong Q-dependence, and can be associated with a translational diffusive process. Γ_{slow} is discernibly and consistently smaller in P(VDF-TrFE) than in PVDF below T_c. Γ_{slow} saturates at higher Q, indicating that the diffusion process consists of jumps. Furthermore, it can be noted that the Γ_{slow} does not approach zero at Q = 0, indicating diffusion within a restricted volume. Adapting the model described in literature,[21,34–36] Γ_{slow} can be described as jump diffusion with Gaussian distribution of jump lengths

$$\Gamma_{slow}(Q) = \frac{1}{\tau}\left[1 - \exp\left(-\frac{Q^2 r_0^2}{2}\right)\right], \tag{3}$$

where τ corresponds to the characteristic time of the jumps and r_0 is the average jump length. The corresponding diffusion coefficient is $D = \frac{r_0^2}{2\tau}$. The observed temperature dependent τ and D values for the two polymers are summarized in Figure 5. While D appear to be comparatively similar in both samples, the characteristic relaxation times τ are consistently larger in the 70/30 P(VDF-TrFE) copolymer at all temperatures investigated. In general, the observed jump length, r_0 is longer in the copolymer than in the bare PVDF. We argue that due to an increase in the unit cell volume in the polar all-T phase, which is caused by the bulkier TrFE monomers,[37] there is an increase in the spacing of the proton jump sites and consequently an extension of their jump time. Above T_c, where there is no preferential configuration between the T- and G bonds and both polymers still maintain their semi-crystalline nature, τ becomes comparable. This suggests a connection between the all-T configuration and the observed dynamics retardation in the copolymer below T_c.

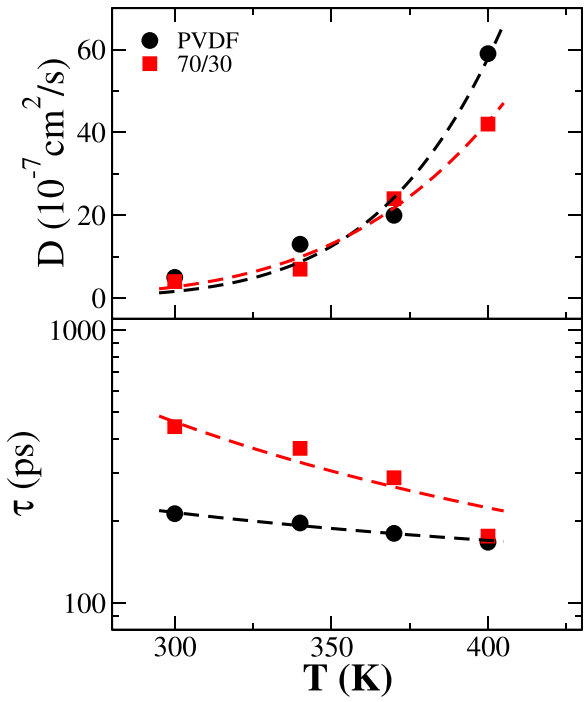

FIG. 5. Top panel: Observed diffusion coefficients as a function of temperature for the two polymer samples. Bottom panel: Corresponding relaxation times.

Using QENS, we have identified two characteristic diffusive processes in PVDF-based copolymers. We have found a connection between the temperature-dependent molecular jump length r_0 and molecular configurations that is set by molar ratio and ferroelectricity. The proton jump lengths become longer in the ferroelectric phase, when compared to the paraelectric phase, due to larger spacing between the jump sites. While the appearance of ferrolectric domains below T_c does not appear to affect the effective proton diffusion at the investigated time scales, the value of T_c clearly depends on the size of the domains which in turn depends on the molar ratio of copolymerization. We conclude that fundamental characteristics of proton diffusions such as the jump length, not typically considered, can be used to better understand ferroelectric properties of polymeric PVDF materials as it is directly related to their dynamic properties.

The authors would like to thank R. Goyette and R. Mills for their excellent technical support during the neutron measurements. AP acknowledges funding support from City University of Hong Kong. Work at ORNL's Spallation Neutron Source is sponsored by the Scientific User Facilities Division, Office of Basic Energy Sciences, U.S. Department of Energy.

[1]Q. M. Zhang, V. Bharti, and X. Zhao, Science **280**, 2101 (1998).
[2]B. Chu, X. Zhou, K. Ren, B. Neese, M. Lin, M. Q. Wang, F. Bauer, and Q. M. Zhang, Science **313**, 334 (2006).
[3]V. V. Kochervinskii, Crystallogr. Rep. **48**, 649 (2003).
[4]S. Zhang, R. Klein, K. Ren, B. Chu, X. Zhang, J. Runt, and Q. M. Zhang, J. Mater. Sci. **41**, 271 (2006).
[5]S. H. Bae, O. Kahya, B. K. Sharma, J. Kwon, H. J. Cho, B. Ozyilmaz, and J.-H. Ahn, ACS Nano **7**, 3130 (2013).
[6]S. Cha, S. M. Kim, H. Kim, J. Ku, J. I. Sohn, Y. J. Park, B. J. Song, M. H. Jung, E. K. Lee, B. L. Choi, J. J. Park, Z. L. Wang, J. M. Kim, and K. Kim, Nano Lett. **11**, 5142 (2011).
[7]L. Persano, C. Dagdeviren, C. Maruccio, L. De Lorenzis, and D. Pisignano, Adv. Mater. **26**, 7574 (2014).
[8]M. Li, I. Katsouras, C. Piliego, G. Glasser, I. Lieberwirth, P. W. M. Blom, and D. M. de Leeuw, J. Mater. Chem. C **1**, 7695 (2013).
[9]H. Su, A. Strachan, and W. A. Goddard, Phys. Rev. B **70**, 064101 (2004).
[10]D. Li, J. Xiong, Y. Guo, and G. Li, J. Appl. Phys. **115**, 204106 (2014).
[11]M. Bohlen and K. Bolton, Phys. Chem. Chem. Phys. **16**, 12929 (2014).
[12]T. Furukawa, Phase Transitions **18**, 143 (1989).
[13]C. Ang and Z. Yu, Adv. Mater. **16**, 979 (2004).
[14]R. G. Kepler and R. A. Anderson, J. Appl. Phys. **49**, 4490 (1978).
[15]S. Ikeda, H. Kominami, K. Koyama, and Y. Wada, J. Appl. Phys. **62**, 3339 (1987).
[16]M. Kobayashi, K. Tashiro, and H. Tadokoro, Macromoelcules **8**, 158 (1975).
[17]K. Tashiro, Y. Itoh, M. Kobayashi, and H. Tadokoro, Macromolecules **18**, 2600 (1985).
[18]K. Tashiro, M. Kobayashi, and H. Tadokoro, Macromolecules **14**, 1757 (1981).
[19]J. Colmenero, A. Arbe, and A. Alegria, Phys. Rev. Lett. **71**, 2603 (1993).
[20]B. Frick, D. Richter, W. Petry, and U. Buchenau, Z. Phys. B. **70**, 73 (1988).
[21]E. Lopez Cabarcos, F. Batallan, B. Frick, T. A. Ezquerra, and F. J. Balta Calleja, Phys. Rev. B **50**, 13214 (1994).
[22]J. F. Legrand, B. Frick, M. Meurer, V. H. Schmidt, M. Bee, and J. Lajzerowick, Ferroelectrics **109**, 321–326 (1990).
[23]T. Furukawa, K. Nakajima, and Y. Takahashi, IEEE Trans. Dielectr. Electr. Insul. **13**, 1120 (2006).
[24]F. Ishii, A. Odajima, and H. Ohigashi, Polym. Prepr. Jpn. **31**, 2325 (1982).
[25]E. Mamontov and K. W. Herwig, Rev. Sci. Instrum. **82**, 085109 (2011).
[26]P. A. Jacobson, Luis G. Rosa, C. M. Othon, K. Kraemer, A. V. Sorokin, S. Ducharme, and P. A. Dowben, Appl. Phys. Lett. **84**, 88–90 (2004).
[27]W. B. Hu, W. J. Hu, Y. A. Liu, J. S. Li, B. Jiang, and K. Wen, Sci. Rep. **4**, 4772 (2014).
[28]See http://www.piezotech.fr/image/documents/22-31-32-33-piezotech-piezoelectric-films-leaflet.pdf.
[29]J. Kaszynska, B. Hilczer, and P. Biskupski, Polym. Bull. **68**, 1121–1134 (2012).
[30]C. N. Borca, B. Xu, T. Komesu, H. Jeong, M. T. Liu, S.-H. Liou, P. A. Fridkin, H. You, and P. A. Dowben, Phys. Rev. Lett. **83**, 4562 (1999).
[31]E. Lopez Cabarcos, A. F. Braña, B. Frick, and F. Batallan, Phys. Rev. B **71**, 184304 (2005).
[32]E. Lopez Cabarcos, A. F. Brana, B. Frick, and F. Batallan, Phys. Rev. B **65**, 104110 (2002).
[33]M.-C. Bellissent-Funel, S. H. Chen, and J.-M. Zanotti, Phys. Rev. E **51**, 4558 (1995).
[34]P. L. Hall and D. K. Ross, Mol. Phys. **42**, 673 (1981).
[35]F. Volino and A. J. Dianoux, Mol. Phys. **41**, 271 (1980).
[36]A. J. Dianoux, M. Pineri, and F. Volino, Mol. Phys. **46**, 129 (1982).
[37]Y. Abe and K. Tashiro, J. Polym. Sci. B: Polym. Phys. **39**, 689 (2001).